Chemical Engineering Journal 109 (2005) 123–131

Chemical Engineering Journal

www.elsevier.com/locate/cej

Variation of the local effective axial dispersion coefficient with bed height in expanded beds

Junxian Yun, Shan-Jing Yao *, Dong-Qiang Lin

Department of Chemical and Biochemical Engineering, Zhejiang University, Hangzhou 310027, PR China

Received 8 July 2004; received in revised form 11 March 2005; accepted 30 March 2005

Abstract

The local axial dispersion characteristics are very important and fundamental for the analyzing, modeling and understanding of biomolecules adsorption performance in expanded bed adsorption. In this work, the local effective axial dispersion coefficients along the bed height of an expanded bed system with porous adsorbent particles, Streamline SP and DEAE, were determined by measuring residence time distributions (RTDs) using the tracer pulse–response method combining in-bed sampling technique. The decreasing trend of the local effective axial dispersion coefficient with the increase of bed height was identified. An empirical correlation for the variations of the local effective axial dispersion coefficient with bed height was developed by taking account of the complex effects of liquid and particle properties, liquid flow behaviors, particle movements and the local bed voidage and particles size variations.

Keywords: Expanded bed adsorption; Axial dispersion; Residence time distribution; Correlation

1. Introduction

Expanded bed adsorption (EBA) is a novel chromatography technique for separation and purification of biological products directly from whole-cell fermentation broths or homogenates without using centrifugation, microfiltration and other clarification prior steps [1–4]. The axial dispersion in EBA is of great importance to reveal the flow performance, to interpret the adsorption and transfer mechanisms of biomolecules and to describe the particular adsorption behaviors along the bed. Due to the broad size and/or density distributions of adsorbent particles used in EBA, non-uniform axial distributions of particle size and local bed voidage are always established within the bed [5–8], which results in the variation of the axial dispersion with bed height.

Several experimental studies have been explored to reveal the overall axial dispersion characteristics in expanded beds [5,9–19], while only a few studies were focused on the local axial dispersion behaviors. Bruce and Chase examined the axial and radial dispersion performance of Streamline SP and DEAE particles by measuring residence time distributions (RTDs) at different in-bed sampling ports located along the bed height [6]. They stated that the top zone of bed had lower axial dispersion than the bottom region by analyzing the obtained values of Bodenstein number in different zones from the inlet distribution plate to the various positions in the bed. The increasing trends of theoretical plate number in the bed zone from the bed inlet to a certain height position with the increase of bed height were also observed for Streamline SP and DEAE particles in our previous work [19]. Unfortunately, it is quite vague and not accurate to describe the local axial dispersion behaviors using Bodenstein number and theoretical plate number obtained in the bed zones from the bed inlet to each certain height position. In addition, since porous adsorbent particles are widely applied in EBA, axial dispersion occurs not only in the bed voids between particles but also within pores of particles. Therefore, the local effective axial dispersion coefficient is of interest in describing the local axial dispersion characteristics in EBA system. Recently, we measured the axial dispersion coefficient along the bed height in expanded beds for UpFront FastLine SP adsorbents with a density difference and a log-normal size distribution using the tracer pulse–response method combining in-bed

* Corresponding author. Tel.: +86 571 87951982; fax: +86 571 87951015.
E-mail address: yaosj@che.zju.edu.cn (S.-J. Yao).

1385-8947/$ – see front matter © 2005 Elsevier B.V. All rights reserved.
doi:10.1016/j.cej.2005.03.015

Nomenclature

AE_i	fitting averaged error in the ith zone
c	tracer concentration (mol m^{-3})
C	recorded response signals of tracer concentration (mV)
d_c	inner diameter of column (m)
d_s	particle diameter (m)
d_{smi}	mean particle size in the ith zone (m)
D_{axc}	correlated axial dispersion coefficient (m^2 s^{-1})
D_{axe}	experimental axial dispersion coefficient (m^2 s^{-1})
D_{axi}	local effective axial dispersion coefficient in the ith zone (m^2 s^{-1})
$E()$	residence time distribution function
$F(s)$	transfer function in Laplace domain
g	gravitational acceleration (m s^{-2})
Ga_i	Galileo number in the ith layer defined by Eq. (14)
h	axial bed height (m)
h_{mz}	the middle height of column zone (m)
H	expanded bed height (m)
H_{sb}	settled bed height (m)
Re_{mfi}	onset Reynolds number in the ith zone given by Eq. (13)
Re_{si}	particle Reynolds number in the ith layer defined by Eq. (11)
s	Laplace transformation parameter
S.D.$_i$	fitting standard deviation in the ith zone
t	time (s)
u_i	interstitial liquid velocity in the ith zone (m s^{-1})
u_{i0}	interstitial velocity without taking account the particle porosity in the ith zone (m s^{-1})
u_{i1}	interstitial velocity taking account of particle porosity in the ith zone (m s^{-1})
U_L	superficial liquid velocity (m s^{-1})
x	axial position in expanded bed (m)
x_i	axial position from bed bottom to the inlet of the ith zone (m)
x_{i+1}	axial position from bed bottom to the outlet of the ith zone (m)

Greek letters

β_{0i}	energy dissipation rate per unit mass of liquid neglecting wall resisting in the ith zone (m^2 s^{-3})
β_i	energy dissipation rate per unit mass of liquid in the ith zone (m^2 s^{-3})
β_{ri}	relative energy dissipation rate in the ith zone
$\delta(t)$	Dirac delta function, $\delta(t) = 1$ at $t = 0$ and $\delta(t) = 0$ at $t > 0$
φ_i	local voidage in the ith zone
φ_p	particle porosity
μ_L	liquid viscosity (Pa s)
ρ_L	liquid density (kg m^{-3})
ρ_s	mean particle density (kg m^{-3})
ψ	object function defined by Eq. (7)

sampling technique [20]. A remarkable decreased trend of the local axial dispersion coefficient along the bed height was observed. An empirical correlation for the variations of the local effective axial dispersion coefficients was obtained based on the hydrodynamic performances within the bed.

This work will present the measurements of the local effective axial dispersion coefficients in the different zones along the bed height for Streamline adsorbent particles, which have normal size distributions and relatively uniform densities. The theoretical analysis of the method and the semi-empirical correlation for the local effective axial dispersion in these regions will also be presented.

2. Experimental

2.1. Column and adsorbent

The EBA system and devices used in this work are same as that used in our previous work [20]. The glass expanded bed column is 20 mm in inner diameter and 80 cm in height. A home-made fluid distribution unit was placed at the column bottom and a net adapter at the column top. The fluid distribution unit is a gift from Heinrich-Heine University Düsseldorf, Germany, as used by Lin et al. [21,22]. A small amount of glass beads (0.5 mm diameter, <2% of the settled bed height) was added to distribute the fluid uniformly at the inlet of the column. The column was divided into 13 zones by 13 2.5-mm sampling holes located with about 5 cm intervals along the bed height. These holes were sealed by the moveable rubber bands and a metal sampling needle was inserted in to the column through these holes. The tip of the sampling needle (0.8 mm o.d., 0.5 mm i.d. and 50 mm long) was covered with metal mesh to allow the removal of liquid from the column but prevent the withdrawal of adsorbent particles. The sampling needle was connected to an on-line flow-through UV spectrometer (KNAUER WellChrom fast scanning spectrophotometer K-2600, Berlin, Germany) at 240 nm. A peristaltic pump was connected to the outlet of the UV spectrometer to transfer the liquid at a constant flow rate. The tracer concentration in the fluid was determined by the UV absorbance data, which was fed to an A/D transformer and recorded by a personal computer. A motor valve (Knauer, Berlin, Germany) with a 0.5 ml sample loop was connected to the bottom inlet of the column and used to inject the trace pulses. The axial particle size and local voidage distributions at these ports

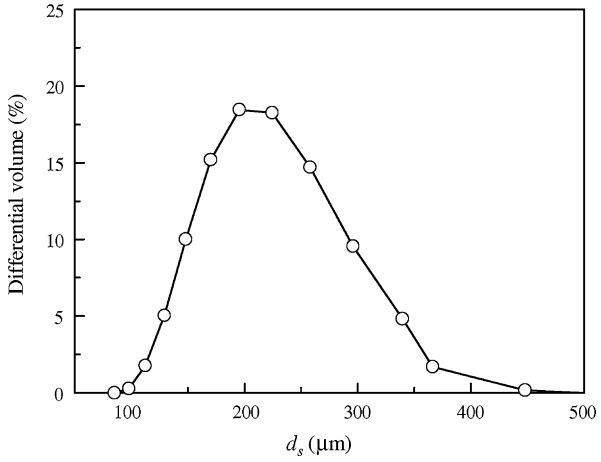

Fig. 1. Particle size distribution of Streamline DEAE.

were also measured by in-bed sampling method, as described previously [7,8].

The adsorbents used here are Streamline SP and DEAE (Amersham Biosciences, Uppsala, Sweden). Size distributions of these particles were measured using Malvern Mastersizer 2000 (Malvern Instruments, Malvern, UK). The particle size of Streamline SP was found in the range of about 90–450 μm and the mean size of 190 μm, as reported in reference [7]. The particle size of Streamline DEAE used here was in the range of 100–450 μm and the mean size of 217 μm, as shown in Fig. 1. These values are slightly different from that of 100–300 μm for size range and 200 μm for mean size stated by the manufacturer, respectively. The mean densities of Streamline SP and DEAE particles are 1184 and 1199 kg m^{-3} (measured using pycnometer), respectively.

2.2. Measurement method

The bed of Streamline DEAE particles was expanded with 50 mM NaH_2PO_4/Na_2HPO_4 buffer (pH 7.2), while the bed of Streamline SP particles was expanded to a stable height with the buffer of 20 mM NaH_2PO_4/Na_2HPO_4 (pH 7.2) and 20% glycerol (w/w). Since Streamline SP and DEAE particles are very similar in particle size distribution, density and porosity, the axial dispersion characteristics of these particles are expected to be similar. Here, we used glycerol added in the buffer for expanding Streamline SP particles, as well as operated in 25 and 30° C, in order to investigate the effects of liquid viscosity. RTDs in various zones along the bed height were obtained by pulse tracer method, which was carried out by introducing an instantaneous pulse (0.5 ml) of tracer (10%, v/v, acetone) from the bottom inlet into the column and then measuring the response signals at the corresponding column positions. At an interest port, the liquid was withdrawn at a constant rate of 0.5 ml min^{-1}, through the sampling needle and the UV spectrometer by the peristaltic pump. The UV absorbance signal of the withdrawn liquid was then measured. The above measurement procedures were repeated in each of the ports one by one. Finally, the obtained RTDs at each region were used to determine the mean local effective axial dispersion coefficients in the corresponding zone along bed height. The experimental and operation conditions are summarized in Table 1.

2.3. Determination of the local effective axial dispersion coefficient

In general, liquid dispersion behaviors in expanded beds are described approximately by plug flow dispersion model assuming a constant axial dispersion coefficient. The axial dispersion coefficient can be determined by measuring the outlet response of an instantaneous pulse injected at the bottom inlet of the column, as similar as the case in fixed beds. Some expressions have be reported for calculating the overall axial dispersion coefficient in expanded beds at various boundary conditions, such as the close–close boundary [5,11,12,17,18], the close–open or open–close boundary [6,19] and the open–open boundary [10,15]. For a stable expanded bed, the axial dispersion varies actually with the increase of bed height due to the axial variations of particle size and voidage, and then cannot be described accurately using the overall axial dispersion coefficient. It is, therefore, necessary to determine the local axial dispersion coefficients along the bed height. In addition, in order to concern with the protein adsorption in expanded bed using porous adsorbent in the future work, here we only consider the case of the local effective axial dispersion coefficient due to porous adsorbent particles used.

Table 1
Operation conditions in tracer pulse experiments

Particles	Liquid	Settled bed height H_{sb} (m)	Expanded bed height H (m)	H/H_{sb}	Superficial liquid velocity (m s^{-1})	Temperature (°C)
DEAE	50 mM phosphate buffer	0.185	0.417	2.25	8.49×10^{-4}	25
		0.190	0.460	2.42	1.17×10^{-3}	25
		0.190	0.565	2.97	1.78×10^{-3}	25
SP	20 mM phosphate buffer and glycerol (20%, w/w)	0.171	0.370	2.16	3.98×10^{-4}	25
		0.171	0.445	2.60	5.84×10^{-4}	30
		0.163	0.540	3.31	7.17×10^{-4}	25

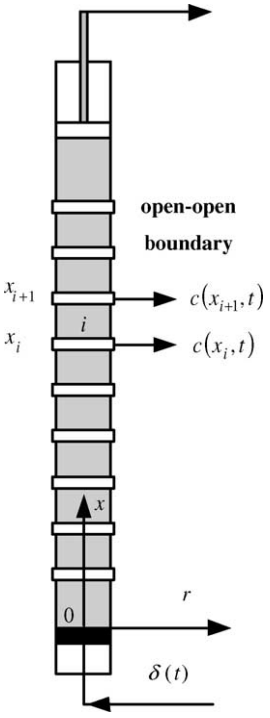

Fig. 2. Schematic of tracer pulse and responses at the inlet and outlet of the ith zone in expanded bed.

As we know, it is difficult to theoretically determine or experimentally examine the continuous variation of the local effective axial dispersion along the bed height due to its complexity. In order to simplify the problem, the expanded bed can be divided into several zones along the bed height [20]. In each zone, both of the liquid velocity and the local effective axial dispersion coefficient are assumed to be constant and the plug flow dispersion model is then available. Therefore, any change of the local effective axial dispersion coefficients in these zones can be considered as an approximation of the actual axial dispersion variation along the bed height. Based on this approximation, the local effective axial dispersion coefficients of these zones can be determined by measuring the RTDs responses at the inlet and outlet of each zone.

A tracer pulse $\delta(t)$, described using Dirac delta function, is injected at the bottom inlet of the column, and the inlet response $c(x_i, t)$ and the output $c(x_{i+1}, t)$ of the ith zone are recorded, as shown schematically in Fig. 2. The governing differential equation for axial dispersion in the ith zone can be expressed as [20]

$$D_{\mathrm{ax}i}\frac{\partial^2 c(x,t)}{\partial x^2} - u_i\frac{\partial c(x,t)}{\partial x} = \frac{\partial c(x,t)}{\partial t} \tag{1}$$

where c is the tracer concentration, $D_{\mathrm{ax}i}$ the local effective axial dispersion coefficient and u_i is the interstitial liquid velocity in the ith zone (including liquid out and within particles), respectively. The initial and boundary conditions are as following:

$$c(x,t)|_{x=0,t=0} = \delta(t) \tag{2}$$

$$c(x,t)|_{x>0,t=0} = 0 \tag{3}$$

$$\lim_{x\to\infty,t>0} c(x,t) = 0 \tag{4}$$

With the given conditions of Eqs. (2)–(4), Eq. (1) can be solved in the Laplace domain using the following transfer function, as similar as that in liquid fluidized beds or packed beds [23–25].

$$F(s) = \frac{c(x_{i+1},s)}{c(x_i,s)} = \exp\left[\frac{x_{i+1}-x_i}{2D_{\mathrm{ax}i}}(u_i - \sqrt{u_i^2 + 4sD_{\mathrm{ax}i}})\right] \tag{5}$$

The output concentration of the ith zone in the time domain is given by inverting Eq. (5) using convolution integral

$$c(x_{i+1},t)_{\mathrm{cal}} = \int_0^t c(x_i,\tau)\frac{x_{i+1}-x_i}{2\sqrt{\pi D_{\mathrm{ax}i}(t-\tau)^3}} \times \exp\left[\frac{u_i(x_{i+1}-x_i)}{2D_{\mathrm{ax}i}}\right] \times \exp\left[-\frac{u_i^2(t-\tau)^2 + (x_{i+1}-x_i)^2}{4D_{\mathrm{ax}i}(t-\tau)}\right] \mathrm{d}\tau \tag{6}$$

Then, the output concentration $c(x_{i+1}, t)_{\mathrm{cal}}$ of the ith zone can be calculated by the given experimental input concentration $c(x_i, t)$ (expressed by the recorded response signals $C(x_i, t)$). The unknown two parameters, $D_{\mathrm{ax}i}$ and u_i, can be determined by fitting the calculated response $C(x_{i+1}, t)_{\mathrm{cal}}$ based on $C(x_i, t)$ with the experimental response $C(x_{i+1}, t)$. The object function $\psi(D_{\mathrm{ax}i}, u_i)$ for the fitting is given by

$$\psi(D_{\mathrm{ax}i}, u_i) = \min\sum_j^M [C(x_{i+1},t)_{\mathrm{cal},j} - C(x_{i+1},t)_j]^2 \tag{7}$$

where M is the number of experimental data.

The solving of Eq. (7) is a two-parameter non-linear least-squares problem, also belongs to unconstrained minimization optimization problems. Here, the solving procedure was simplified by limiting the interstitial liquid velocity u_i into a suitable range. Since Streamline particles have a normal size distribution and an approximately uniform density, we can then calculate the mean particle size and local bed voidage in the ith zone using the model in our previous work [7]. The interstitial velocity is then in the range between the velocities with and without taking account of particle porosity

$$u_{i1} \le u_i \le u_{i0} \tag{8}$$

where u_{i0} is the interstitial velocity without taking account of particle porosity (u_{i0}=U_{L}/φ_i, U_{L} is the superficial liquid velocity) and u_{i1} the interstitial velocity with taking account of particle porosity ($u_{i1} = U_{\mathrm{L}}/\left|\varphi_i + \varphi_{\mathrm{p}}(1-\varphi_i)\right|$), respectively. The particle porosity φ_{p} is 0.84 for Streamline SP, and 0.85 for Streamline DEAE obtained by measuring the volume of water saturated within the particles, i.e. measuring the weights of the given-volume wet and dry particles. Then,

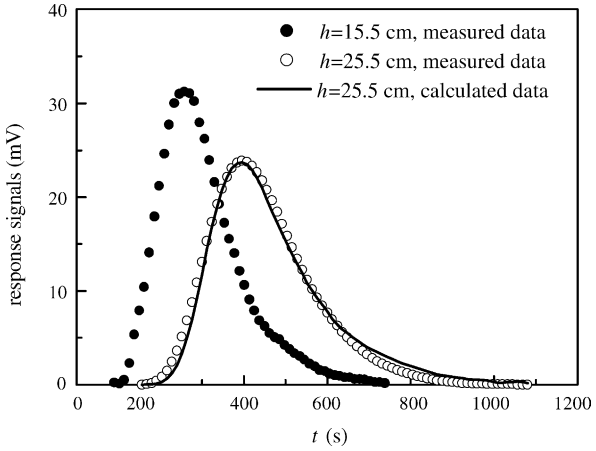

Fig. 3. Comparison of the experimental and fitted pulse–response signals. (Streamline SP, $u_i = 6.88 \times 10^{-4}$ m s^{-1}, $D_{axi} = 7.89 \times 10^{-6}$ m^2 s^{-1}, $H_{sb} = 17.1$ cm, $H = 44.5$ cm, S.D.$_i = 3.28\%$, AE$_i = 8.91\%$).

the unconstraint optimization problem of solving Eq. (7) now can be transferred to the constraint optimization problem by restricting the variables u_i using Eq. (8). The algorithm of trust region method based on the interior-reflective Newton method [26,27] was employed to determine the unknown parameters D_{axi} and u_i.

The responses of tracer pulses at the inlet and the outlet of each zone in beds with Streamline SP and DEAE particles were obtained at different liquid flow velocities. The original recorded signals of the responses were smoothed to remove the random noise. Then, the local effective axial dispersion coefficients in different zones were determined by fitting the obtained responses and the corresponding calculated signals. The quality of the fitting was evaluated by the standard deviation, S.D., and the averaged error, AE, as described in reference [20].

Fig. 3 shows an example of the obtained responses in the zone with its bottom inlet at bed height $h_i = 15.5$ cm and its top outlet at $h_{i+1} = 25.5$ cm. The corresponding fitted signals at $h_{i+1} = 25.5$ cm was based on the measured response data at $h_i = 15.5$ cm and compared with the measured response at $h_{i+1} = 25.5$ cm. Streamline SP particles were used here. As shown in Fig. 3, the fitting accuracy is good and the fitted values agree well with the experimental data.

3. Results and discussion

3.1. RTD curves in different column zones

Bruce and Chase presented RTD curves at several heights in the column for Streamline SP and DEAE particles [6]. The beds were expanded to two times of settled bed heights with NaH_2PO_4 buffer. In this work, we have measured RTDs at different sampling ports in the bed of Streamline SP particles expanded with 20% glycerol NaH_2PO_4/Na_2HPO_4 buffer at the liquid superficial velocities of 3.98×10^{-4}, 5.84×10^{-4} and 7.17×10^{-4} m s^{-1}, respectively, and Streamline DEAE particles with 50 mM NaH_2PO_4/Na_2HPO_4 buffer at the liquid superficial velocities of 8.49×10^{-4}, 1.17×10^{-3} and 1.78×10^{-3} m s^{-1}. Parts of the obtained RTDs are depicted in Figs. 4 and 5, where $E()$ is the residence time distribution function. As can be seen, the obtained RTD curves near the bottom of bed (from the bottom inlet to the height of about 10–15 cm) developed in a serious unsymmetrical shape with extended tail, which indicates that the dispersion and mixing are intensive in these regions. These behaviors are similar to those reported by Bruce and Chase [6] and by Yun et al. [19]. With the increase of bed height, however, RTD curves become more regular and symmetrical than those in the bottom zones, which indicate that the dispersion and mixing become a slightly weaker near the bed top, especially in the region between the outlet of the bed and the position of 5–10 cm below the bed top. However, even in the region near the bed top the axial dispersion cannot be ignored, because nearly all the obtained RTDs in the present conditions have extended tails. These results also demonstrate the necessity to quantitate the non-uniform axial dispersion behaviors.

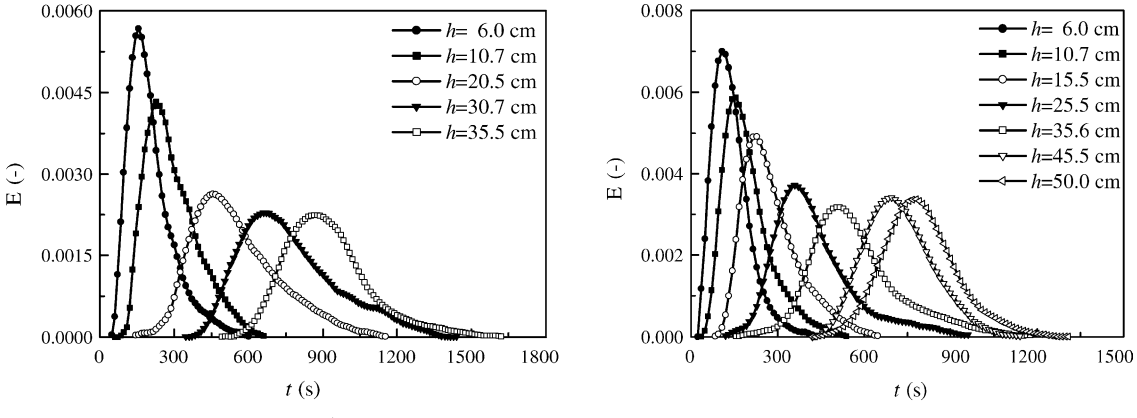

Fig. 4. RTDs at different column heights in the bed of Streamline SP particles.

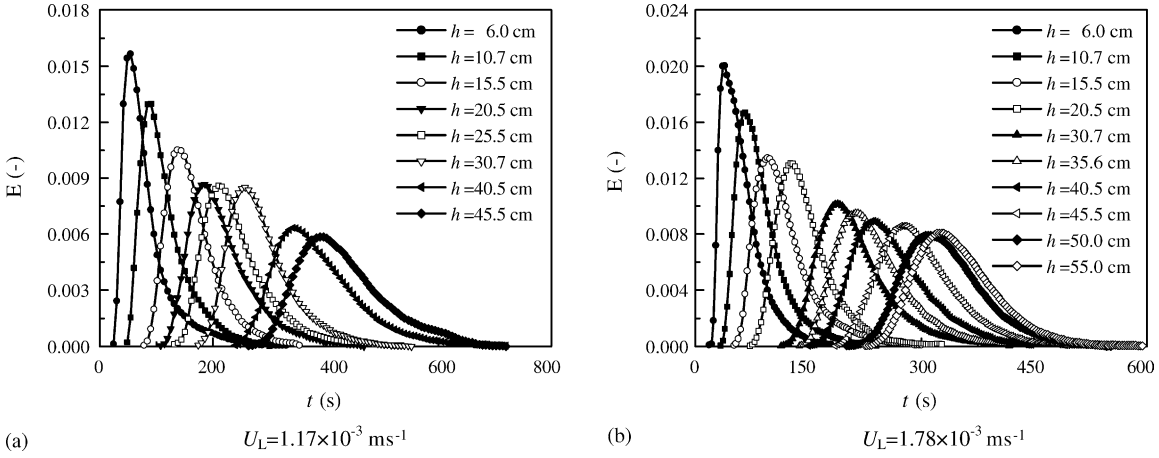

Fig. 5. RTDs at different column heights in the bed of Streamline DEAE particles.

3.2. Axial dispersion characteristics in different column zones

The local effective axial dispersion coefficients in different zones along the bed height were determined by the above fitting method in time domain. During the fitting procedures, axial variations of the local bed voidage under the corresponding conditions were calculated by the model assuming a constant particle density as published previously [7]. The constrained ranges for the interstitial velocity in each interest zone were then estimated based on the mean local voidage values. Eqs. (7) and (8) were employed to calculate the local effective axial dispersion coefficients.

The predicted values for the change of local voidage with bed heights for Streamline SP particles at various liquid superficial velocities are presented in Fig. 6(a). These data were also in agreement well with the experimental data obtained in NaH_2PO_4/Na_2HPO_4 buffer at approximately the same bed expansion degrees [7]. The axial distributions of the local bed voidage for Streamline DEAE particles at different liquid superficial velocities, as well as the measured data by the in-bed sampling method, are presented in Fig. 6(b). Since the densities of Streamline DEAE particles used in this work were broad (in the range of 1125–1313 kg m^{-3}), the model prediction gives a slight deviation of local voidage than the experimental data. Therefore, the experimental values of local voidage were used directly in the fitting processes for Streamline DEAE particles here.

The local effective axial dispersion coefficients in different column zones for Streamline SP and DEAE particles are shown in Fig. 7, where h_{mz} denotes the middle height of column zone describing the axial location of the zone in the column. For Streamline SP, the averaged values of S.D. at the liquid superficial velocities of 3.98×10^{-4}, 5.84×10^{-4} and 7.17×10^{-4} m s^{-1} are 6.9, 4.2 and 7.2% and the averaged values of AE are 14.6, 9.7 and 16.0%. For Streamline DEAE, the averaged values of S.D. at the liquid superficial velocities of 8.49×10^{-4}, 1.17×10^{-3} and 1.78×10^{-3} m s^{-1} are 9.3, 9.7 and 4.3% and the averaged values of AE are 20.8, 20.9 and 8.8%, respectively. It can be seen that the local effective axial dispersion coefficient decrease with increasing the bed height in all interest expansion degrees for Streamline SP particles and at the relatively low liquid superficial velocities of 8.49×10^{-4} and 1.17×10^{-3} m s^{-1} for Streamline DEAE particles. The values of the local effective axial dispersion coefficient in the zones near the bed bottom are higher

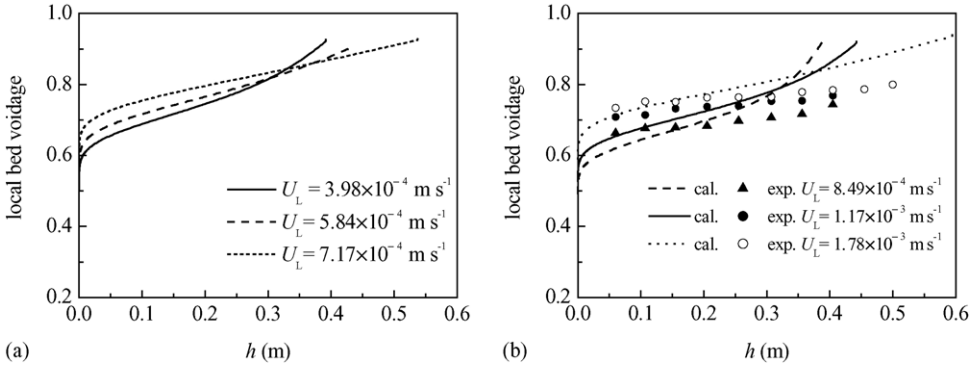

Fig. 6. Axial variations of local bed voidage at different liquid superficial velocities.

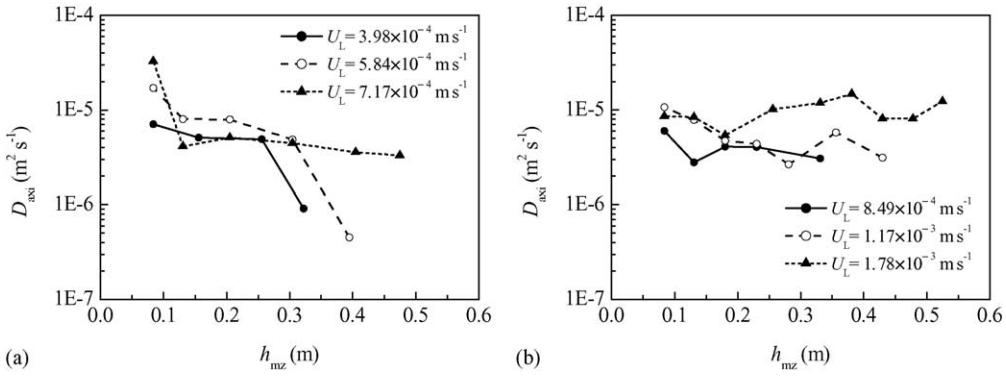

Fig. 7. Variations of the local effective axial dispersion coefficients in different column zones.

obviously than those in the zones with the height higher than 15 cm. The reason is that the bed voidage in these zones are low, as shown in Fig. 6, and the concentrations of the solid particles are high. Therefore, the interactions between particles should be relative intense, which results in the unwanted movements of particles upward and downward in a certain range. In the experimental process, we also observed the falls and rises of particles near the bed bottom, which may aggravate the liquid back-mixing and increase the local effective axial dispersion coefficient. The other reason is the inlet effect, i.e. the non-uniform liquid flow profile at the bed inlet induced by the fluid distributor.

With the increase of bed height, the local effective axial dispersion coefficients decrease for most conditions of Streamline SP and DEAE, as shown in Fig. 7. The reason is that the inlet effect decrease with the increase of bed height and the relative uniform fluid flow upward through the bed exists in these zones. In the zones near the top of bed (5–10 cm below the bed top), low axial dispersion coefficients were observed for Streamline SP at the liquid superficial velocities of 3.98×10^{-4} to 7.17×10^{-4} m s^{-1} and for Streamline DEAE at the liquid superficial velocities of 8.49×10^{-4} and 1.17×10^{-3} m s^{-1}. The other reasons are that the bed voidages in these zones are high and the concentrations of solid particles are low. So, the particles stay stably and the axial dispersion induced by the particle movements is very low, which induces the low axial dispersion.

However, for Streamline DEAE at high liquid superficial velocity of 1.78×10^{-3} m s^{-1}, there is no obvious variation of the local effective axial dispersion coefficient along the bed height. This is because that the liquid buffer has a lower density than that used for Streamline SP particles and the convection is intense and dominant under high liquid superficial velocities, which increase the axial dispersion and mixing along the whole column.

3.3. Correlation of the local effective axial dispersion coefficients

A suitable correlation for axial dispersion coefficient is important and fundamental for modeling the biomolecules adsorption and analyzing proteins breakthrough behaviors in EBA. Although numerous correlations for overall axial dispersion coefficient in liquid–solid fluidized beds have been reported [28–31], there is a lack of correlation for axial dispersion in expanded beds due to the particularity of expanded bed.

The axial dispersion and mixing in expanded beds are affected by the liquid physical properties (density, viscosity, etc.), particle properties (density and size distributions, averaged diameter and density, porosity, etc.), operation conditions (liquid flow velocity, temperature, settled bed height, etc.), column conditions (column diameter, length, inlet distribution, etc.) and other variables. Therefore, it is difficult to take account of all variables mentioned above in the correlation of the local effective axial dispersion coefficient in EBA columns. Recently, we obtained an empirical correlation of the local effective axial dispersion coefficients for UpFront FastLine SP adsorbents with a density difference and a log-normal size distribution [20]. We considered three parts of the contributions to the variation behaviors of the local effective axial dispersion coefficient in expanded beds: (a) the variations of local voidage, (b) the effects of interstitial velocity and properties of liquid and particles and (c) the particle movement due to the particle–particle interactions and the near-wall non-uniform velocity profile. The former two factors can be described using the local voidage and particle Reynolds number, while the latter can be described by employing the relative energy dissipation rate. For Streamline particles used in this work, the contributions to the variation behaviors of the local effective axial dispersion coefficient with bed height can also be divided into three parts as mentioned above. Then, the local effective axial dispersion coefficient can be described as the function of the corresponding three variables. The experimental values of the local effective axial dispersion coefficient for Streamline SP and DEAE particles at the mentioned liquid flow conditions were fitted using the similar non-linear least-squares procedure and the following empirical equation was obtained:

$$\frac{D_{axi}\rho_L}{\mu_L} = 13.2(Re_{si}\varphi_i)^{0.65}\beta_{ri}^{-0.05} \quad (9)$$

where ρ_L is the liquid density, μ_L the liquid viscosity, φ_i the local voidage in the ith zone, β_{ri} is the relative energy dissipation rate expressed as

$$\beta_{ri} = \frac{32U_L}{\frac{d_c^2(\rho_s-\rho_L)(1-\phi_i)\phi_i g}{\mu_L} + 32U_L} \tag{10}$$

and Re_{si} is the particle Reynolds number in the ith zone and given by

$$Re_{si} = \frac{d_{smi}U_L\rho_L}{\mu_L} \tag{11}$$

where d_c is the inner diameter of column, ρ_s is the mean particle density, g is the gravitational acceleration, d_{smi} is the mean particle size in the ith zone.

The ranges of these parameters are $0.03 \le Re_{si} \le 0.5$, $0.66 \le \varphi_i \le 0.90$, $1.4\times10^{-4} \le \beta_{ri} \le 7.8\times10^{-4}$. It is also seen that the correlation Eq. (9) for Streamline particles is similar as that for UpFront SP reported previously [20]. From Eq. (9), in the case of $\varphi_i = 1$, no particles stay in the column and $\beta_{ri} = 1$, then the term of the relative energy dissipation rate will disappear and thus the axial dispersion will only be a function of Reynolds number. In the case of $\varphi_i = 0$, no liquid flow occurs in the column and $D_{axi} = 0$.

Fig. 8 compares the experimental data with those calculated data by Eq. (9). The standard deviation, S.D., and the averaged error, AE, of Eq. (9) in the fitting are 15.6 and 30.1%, respectively. The present correlation was also compared with the correlations for liquid–solid fluidized beds suggested by Chung and Wen [28] and by Kikuchi et al. [30]. For expanded beds considered here, we write these correlations as following [20]:

The correlation by Chung and Wen is expressed as

$$\frac{D_{axi}\rho_L}{\mu_L}\left(\frac{Re_{mfi}}{Re_{si}}\right) = \frac{Re_{si}}{0.20 + 0.011Re_{si}^{0.48}} \tag{12}$$

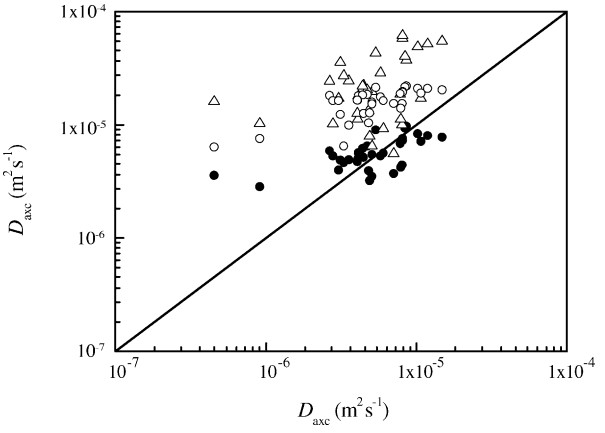

Fig. 8. Comparison of experimental and correlated axial dispersion (D_{axe} and D_{axc}, respectively) and correlations by (Δ) Chung and Wen [28], (◯) Kikuchi et al. [30] and (●) this work.

where Re_{mfi} is the onset Reynolds number in the ith zone given by

$$Re_{mfi} = \sqrt{33.7^2 + 0.0408Ga_i} - 33.7 \tag{13}$$

and Ga_i is Galileo number in the ith layer given by

$$Ga_i = \frac{d_{smi}^3 g(\rho_{si}-\rho_L)\rho_L}{\mu_L^2} \tag{14}$$

The correlation by Kikuchi et al. is written as

$$\frac{D_{axi}\rho_L}{\mu_L} = 500\beta_{0i}^{0.43}\exp[-20.5(0.75-\varphi_i)^2] \tag{15}$$

where β_{0i} is the energy dissipation rate per unit mass of liquid in the ith zone [20].

As can been seen, both correlations by Chung and Wen and by Kikuchi et al. overestimates the axial dispersion coefficients compared with those experimental values, while the present correlation Eq. (9) gives more accurate predictions under the conditions in this work. As pointed in our previous work [20], the reason is that the correlations by Chung and Wen and by Kikuchi et al. are available in describing the overall dispersion in liquid–solid fluidized beds or packed beds and are not suitable to be applied in the zones along the bed height in expanded beds due to the different hydrodynamics. Moreover, bed voidage was not included in the correlation by Chung and Wen and particle size was ignored in the correlation by Kikuchi et al.

The present correlation is expected to be useful in understanding the micro-mechanisms and non-uniform hydrodynamics of liquids in expanded beds, and also useful in determining the local effective axial dispersion coefficients along the bed height for the prediction of adsorption performance in EBA. However, till now this correlation was challenged only for the description of the variations of axial dispersion in the condition that there are no cells or cell debris in liquids. For the real feedstocks with cells or cell debris and for the highly viscous process liquors, the correlation should be improved and detailed studies are still needed.

4. Conclusions

The tracer pulse–response measurement combining in-bed sampling method was used to study the axial dispersion characteristics along bed height in expanded beds. The fitting method in the time domain was developed to determine the local effective axial dispersion coefficients from RTDs data. The obtained values in various zones showed a decreasing trend of the local effective axial dispersion coefficient with the increase of bed height. The dispersion and mixing in the zones near the bed bottom are intense due to the non-uniform flow, the near-wall falls and rises of particles and the higher interstitial liquid velocity. The local effective axial dispersion coefficients near the bed top are quite lower than those of bed

bottom, which indicates that the uniform fluid flow and stable expansion of particles occur in the middle and top of bed.

Correlation for the local effective axial dispersion coefficient in expanded beds was achieved by taking account of the effects of interstitial velocity, the liquid and particle properties, the particle movement and the local voidage and particles size variation. An empirical correlation for the variations of the local effective axial dispersion coefficient in various zones along the bed height was suggested by considering these factors together. The correlation obtained is available for the description of the local axial dispersion variations for Streamline particles expanded with liquid buffer without cells or cell debris in expanded beds, and the further application on the accurate characterization of protein adsorption in expanded bed could be hoped.

Acknowledgments

The support of the National Natural Science Foundation of China (No. 20206029) is gratefully acknowledged. The authors are grateful to the research support from Zhejiang Province Foundation for post-doctors. We also want to thank the German Academic Exchange Service (DAAD) for the instrument donation of Spectrophotometer K2600. The authors are also grateful to the reviewers for their valuable suggestion to enhance this paper.

References

[1] H.A. Chase, Purification of proteins by adsorption chromatography in expanded beds, Trends Biotechnol. 12 (1994) 296.
[2] R. Hjorth, Expanded bed adsorption in industrial bioprocessing: recent developments, Trends Biotechnol. 15 (1997) 230.
[3] J. Thömmes, Fluidized bed adsorption as a primary recovery step in protein purification, Adv. Biochem. Eng. 58 (1997) 185.
[4] F.B. Anspach, D. Curbelo, R. Hartman, G. Garke, W.D. Deckwer, Expanded-bed chromatography in primary protein purification, J. Chromatogr. A 865 (1999) 129.
[5] N.A. Willoughby, R. Hjorth, N.J. Titchener-Hooker, Experimental measurement of particle size distribution and voidage in an expanded bed adsorption system, Biotechnol. Bioeng. 69 (2000) 649.
[6] L.J. Bruce, H.A. Chase, Hydrodynamics and adsorption behaviour within an expanded bed adsorption column studied using in-bed sampling, Chem. Eng. Sci. 56 (2001) 3149.
[7] J.X. Yun, S.-J. Yao, D.-Q. Lin, M.-H. Lu, W.-T. Zhao, Modeling axial distributions of adsorbent particle size and local voidage in expanded bed, Chem. Eng. Sci. 59 (2004) 449.
[8] J.X. Yun, D.-Q. Lin, M.-H. Lu, L.-N. Zhong, S.-J. Yao, Measurement and modeling of axial distribution of adsorbent particles in expanded bed: taking into account the particle density difference, Chem. Eng. Sci. 59 (2004) 5873.
[9] J. Thömmes, M. Halfar, S. Lenz, M.-R. Kula, Purification of monoclonal antibodies from whole hybridoma fermentation broth by fluidized bed adsorption, Biotechnol. Bioeng. 45 (1995) 205.
[10] J. Thömmes, M. Weiher, A. Karau, M.-R. Kula, Hydrodynamics and performance in fluidized bed adsorption, Biotechnol. Bioeng. 48 (1995) 367.
[11] A. Karau, C. Benken, J. Thömmes, M.R. Kula, The influence of particle size distribution and operating conditions on the adsorption performance in fluidized beds, Biotechnol. Bioeng. 55 (1997) 54.
[12] N. Ameskamp, C. Priesner, J. Lehmann, D. Lütkemeyer, Pilot scale recovery of monoclonal antibodies by expanded bed ion exchange adsorption, Bioseparation 8 (1999) 169.
[13] S. Yamamoto, N. Akazaki, O. Kaltenbrunner, P. Watler, Factors affecting dispersion in expanded bed chromatography, Biosepration 8 (1999) 33.
[14] S. Yamamoto, A. Okamoto, P. Watler, Effects of adsorbents properties on zone spreading in expanded beds, Biosepration 10 (2001) 1.
[15] H.-B. Hu, D.-Q. Lin, Z.-J. Ye, L.-H. Mei, S.-J. Yao, Z.-Q. Zhu, Expansion characteristics and liquid mixing performance in expanded bed, J. Chem. Eng. Chin. Univ. 14 (2000) 139 (in Chinese).
[16] E. Palsson, A. Axelsson, P.-O. Larsson, Theories of chromatographic efficiency applied to expanded beds, J. Chromatogr. A 912 (2001) 235.
[17] I. Theodossiou, H.D. Elsner, O.R.T. Thomas, T.J. Hobley, Fluidisation and dispersion behaviour of small high density pellicular expanded bed adsorbents, J. Chromatogr. A 964 (2002) 77.
[18] F. Fenneteau, H. Aomari, P. Chahal, R. Legros, Modeling of scale-down effects on the hydrodynamics of expanded bed adsorption columns, Biotechnol. Bioeng. 81 (2003) 790.
[19] J.X. Yun, D.-Q. Lin, S.-J. Yao, Nonuniform hydrodynamics and axial dispersion behaviors in expanded beds, in: Presented at the Fourth International Conference on Separation Science and Technology, Nanning, China, 2004.
[20] J.X. Yun, D.-Q. Lin, S.-J. Yao, Variation of the axial dispersion along the bed height for adsorbents with a density difference and a log-normal size distribution in an expanded bed, Ind. Eng. Chem. Res. 43 (2004) 8066.
[21] D.-Q. Lin, H.M. Fernández-Lahore, M.R. Kula, J. Thömmes, Minimising biomass/adsorbent interactions in expanded bed adsorption processes: a methodological design approach, Bioseparation 10 (2001) 7.
[22] D.-Q. Lin, M.R. Kula, A. Liten, J. Thömmes, Stability of expanded beds during the application of crude feedstock, Biotechnol. Bioeng. 81 (2003) 21.
[23] S. Wronski, E. Molga, Axial dispersion in packed beds: the effect of particle size non-uniformities, Chem. Eng. Process. 22 (1987) 123.
[24] T. Funazukuri, C. Kong, Kagei, Effective axial dispersion coefficients in packed beds under supercritical conditions, J. Supercrit. Fluids 13 (1998) 169.
[25] T. Renganathan, K. Krishnaiah, Liquid phase mixing in 2-phase liquid–solid inverse fluidized bed, Chem. Eng. J. 98 (2004) 213.
[26] T.F. Coleman, Y. Li, On the convergence of reflective newton methods for large-scale nonlinear minimization subject to bounds, Math. Programm. 67 (1994) 189.
[27] T.F. Coleman, Y. Li, An interior, trust region approach for nonlinear minimization subject to bounds, SIAM J. Optimization 6 (1996) 418.
[28] S.F. Chung, C.Y. Wen, Longitudinal dispersion of liquid flowing through fixed and fluidized beds, AIChE J. 14 (1968) 857.
[29] P.R. Krishnaswamy, R. Ganapathy, L.W. Shemilt, Correlating parameters for axial dispersion in liquid fluidized systems, Can. J. Chem. Eng. 56 (1978) 550.
[30] K.-I. Kikuchi, H. Konno, S. Kakutani, T. Sugawara, H. Ohashi, Axial dispersion of liquid in liquid fluidized beds in the low reynolds number region, J. Chem. Eng. Jpn. 17 (1984) 362.
[31] J.-H. Koh, P.C. Wankat, L.N.-H. Wang, Pore and surface diffusion and bulk-phase mass transfer in packed and fluidized beds, Ind. Eng. Chem. Res. 37 (1998) 228.